Protein Engineering

International Edition: DOI: 10.1002/anie.201804506
German Edition: DOI: 10.1002/ange.201804506

In Situ Cyclization of Native Proteins: Structure-Based Design of a Bicyclic Enzyme

*Marta Pelay-Gimeno, Tanja Bange, Sven Hennig, and Tom N. Grossmann**

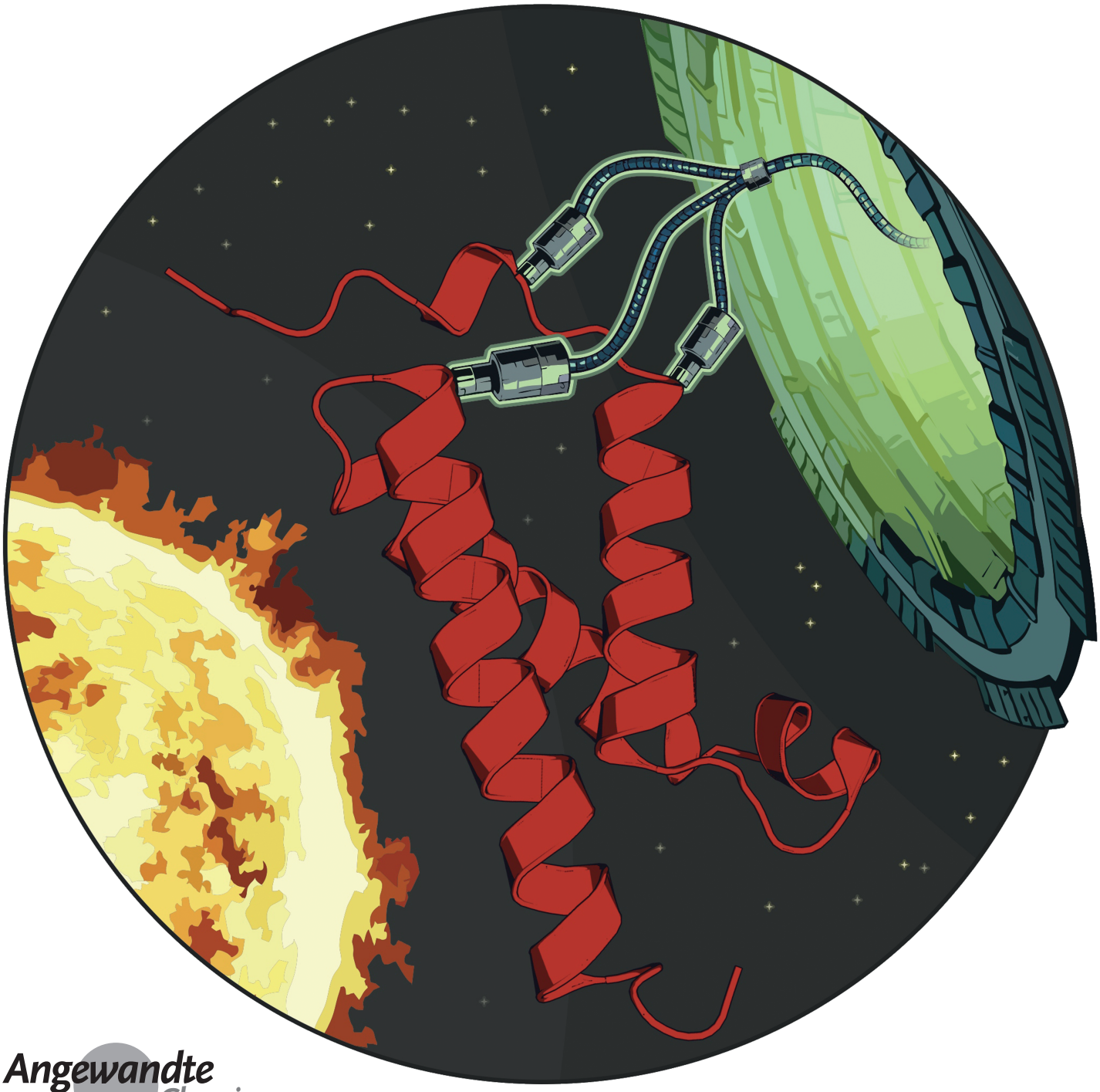

Abstract: *Increased tolerance of enzymes towards thermal and chemical stress is required for many applications and can be achieved by macrocyclization of the enzyme resulting in the stabilizing of its tertiary structure. Thus far, macrocyclization approaches utilize a very limited structural diversity, which complicates the design process. Herein, we report an approach that enables cyclization through the installation of modular crosslinks into native proteins composed entirely of proteinogenic amino acids. Our stabilization procedure involves the introduction of three surface-exposed cysteine residues, which are reacted with a triselectrophile, resulting in the in situ cyclization of the protein (INCYPRO). A bicyclic version of sortase A was designed that exhibits increased tolerance towards thermal as well as chemical denaturation, and proved to be efficient in protein labeling under denaturing conditions. In addition, we applied INCYPRO to the KIX domain, resulting in up to 24°C increased thermal stability.*

Enzymes are an essential component of most biotechnological and biomedical processes[1] but their scope of application is hampered by a limited stability under often desired harsh conditions (e.g., elevated temperature or presence of denaturants). Consequently, the stabilization of protein structures is essential when developing suitable enzymes. The complexity of interactions in protein tertiary structures and the sensitivity of enzymatic activity towards sequence alterations render enzyme stabilization very challenging. A minimally invasive strategy involves the use of covalent protein modifications (e.g., PEGylation or glycosylation) being mainly applied to increase biostability for therapeutic applications.[2] Alternatively, enzyme stabilization can be achieved by sequence variation through directed evolution, consensus-based mutagenesis, or computational approaches,[3] which can be complemented by the introduction of non-proteinogenic amino acids.[4] These approaches aim for improved protein core interactions, structure rigidification, and/or surface charge redistribution, and often require multiple rounds of optimization to achieve relevant stabilization.

[*] Dr. M. Pelay-Gimeno, Dr. S. Hennig, Prof. Dr. T. N. Grossmann
Department of Chemistry & Pharmaceutical Sciences
VU University Amsterdam
De Boelelaan 1108, 1081 HZ, Amsterdam (The Netherlands)
E-mail: t.n.grossmann@vu.nl
Dr. T. Bange
Department of Mechanistic Cell Biology
Max-Planck Institute of Molecular Physiology
Otto-Hahn-Str. 11, 44227 Dortmund (Germany)
and
Department for Systems Chronobiology, LMU Munich
Goethe-Str. 31, 80336 Munich (Germany)
Supporting information and the ORCID identification number(s) for the author(s) of this article can be found under: https://doi.org/10.1002/anie.201804506.

The stabilization of enzymes has also been achieved by the introduction of intramolecular crosslinks. Early examples involve the installation of additional disulfide bridges,[5] which was later complemented by disulfide mimics that are insensitive to reducing environments.[6] Stabilization by disulfides is challenging, in particular when replacing residues in the protein core, as this can cause the loss of non-covalent interactions, thereby reducing the benefit of crosslinking.[7] For that reason, the incorporation of disulfides into flexible protein regions and on the protein surface proved more successful. However, the short distance of the disulfide bridge limits its applicability.[8] Alternatively, the crosslinking of protein termini through lactam formation was applied,[9] requiring a suitable spatial alignment of the N- and C-termini. To reduce these structural prerequisites, the incorporation of non-natural amino acids was pursued to enable crosslinking with an appropriately aligned cysteine side chain.[10] However, the necessity of amber stop codon suppression for the introduction of these non-natural amino acids complicates protein expression. In addition, the screening of linker libraries is hampered as the incorporation of such modified amino acids requires the evolution of a corresponding tRNA synthetase.[11] Taken together, enzyme stabilization endeavors would greatly benefit from an approach that enables the installation of modular crosslinks into proteins only consisting of natural amino acids.

Herein, we report a structure-based stabilization strategy involving the in situ cyclization of proteins (INCYPRO) composed entirely of proteinogenic amino acids (Figure 1a). Using an initial set of monocyclic enzyme variants, we evaluated the feasibility of crosslinking two intradomain cysteine residues using a biselectrophile. Subsequently, a triselectrophilic crosslinker was employed to generate a bicyclic enzyme with high tolerance towards thermal and chemical stress.

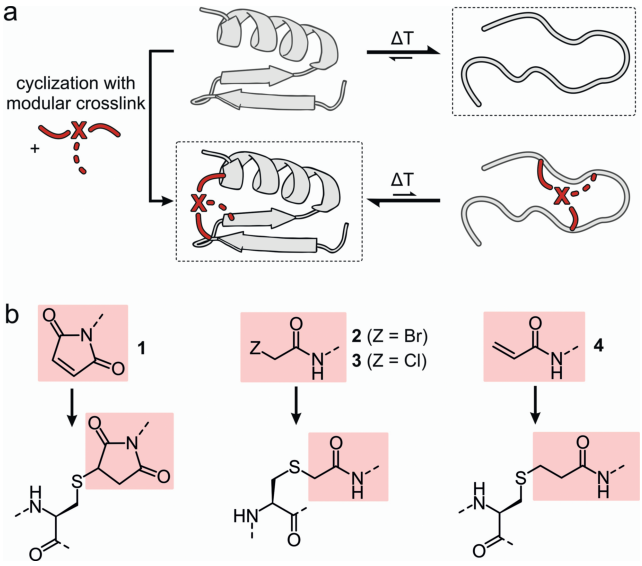

Figure 1. a) Macrocyclization strategy towards stabilized protein tertiary structures using a modular bis- or triselectrophilic crosslink. b) Electrophiles (maleimide **1**, 2-bromoacetamide **2**, 2-chloroacetamide **3**, acrylamide **4**) considered for the crosslinking of accessible cysteines.

We chose *Staphylococcus aureus* sortase A (SrtA, aa 60–206) as the target of our stabilization efforts. SrtA is a transpeptidase and an important biomolecular tool enabling the specific labeling of proteins.[12] The labeling efficiency drops when higher temperatures or denaturants are used, limiting its applicability. To stabilize SrtA, we considered a crosslinking strategy that has previously been applied to constrain peptides and involves the use of biselectrophiles that target pairs of cysteines.[13] Different from these examples, SrtA already contains a cysteine (C184) that is crucial for catalytic activity and may undergo undesired reactions with the electrophile. For that reason, we first tested four electrophiles (**1**–**4**; Figure 1b), previously used for cysteine labeling, regarding their propensity to react with cysteine C184. Reaction conditions suitable for preparative-scale protein modification led to substantial modification of C184 when the enzyme was incubated with maleimide (**1**) and 2-bromoacetamide (**2**), but not for 2-chloroacetamide (**3**) and acrylamide (**4**; see the Supporting Information, Figure S1 and Table S1). These differences in the labeling potential are in line with the electrophilicities of these compounds (**1** > **2** > **3** ≈ **4**).[14] Noteworthy, C184 is shielded by active-site residues, which reduces its general accessibility.[15] As thiols tend to undergo reversible addition to acrylamides, we finally chose 2-chloroacetamide (**3**) as the electrophile for our crosslinkers, which should enable selective labeling of introduced, solvent-exposed cysteines. A set of biselectrophilic linkers with 8–17 bridging atoms (**b1**–**b6**; Figure 2a) spanning a broad range of distances (up to 21 Å, Figure S2) was designed.

Suitable positions for the introduction of cysteine pairs in SrtA were selected to evaluate their suitability for tertiary-structure stabilization. We considered surface residues not involved in substrate recognition and selected pairs that are located in two different secondary structure elements while still being in spatial proximity (distance < 20 Å, based on NMR structure, PDB ID 1ija). Based on these criteria, six SrtA variants (**S1**–**S6**; Figures 2b and S3) were designed, expressed in *E. coli*, and purified. Subsequently, crosslinking reactions with all biselectrophiles were performed, which showed various degrees of conversion. Formation of the cyclization product was confirmed by MS and SDS-PAGE analysis (Figures S4 and S5). While we observed high conversions for **S1**, **S3**, **S4**, and **S6** with all crosslinkers, **S2** and **S5** showed overall high heterogeneity (Figure S4). After the reaction, protein samples were dialyzed to remove unreacted biselectrophiles. Initially, the apparent melting temperatures (T_m) of all unmodified and crosslinked variants (as obtained after dialysis) were determined by changes in tryptophan fluorescence (Figures 2c and S6). Compared to SrtA ($T_m = 59.4\,°C$), all non-crosslinked variants showed a lower thermal stability except for **S3** ($\Delta T_m = +2.9\,°C$). Enzyme crosslinking results in strong stabilization of the cyclic **S3** versions ($\Delta T_m \geq +10.1\,°C$) while more moderate effects were observed for the remaining variants. The most stable versions per variant are **S1-b1** ($\Delta T_m = +2.8\,°C$), **S2-b2** ($\Delta T_m = +0.4\,°C$), **S4-b3** ($\Delta T_m = +4.4\,°C$), **S5-b5** ($\Delta T_m = +3.4\,°C$), and **S6-b1** ($\Delta T_m = +3.9\,°C$).

SrtA is a transpeptidase that cleaves its peptide recognition motif (LPXTG, Figure 2d) to form a thioester intermediate. This intermediate is preferably attacked by the N-terminus of oligoglycine to form a new peptide bond (Figure 2d). In the absence of a suitable nucleophile, water will attack and hydrolyze the thioester (Figure 2d). To investigate enzymatic activity, a previously reported probe system was applied in which a fluorophore/quencher pair is separated upon SrtA processing (Figure S7). For activity

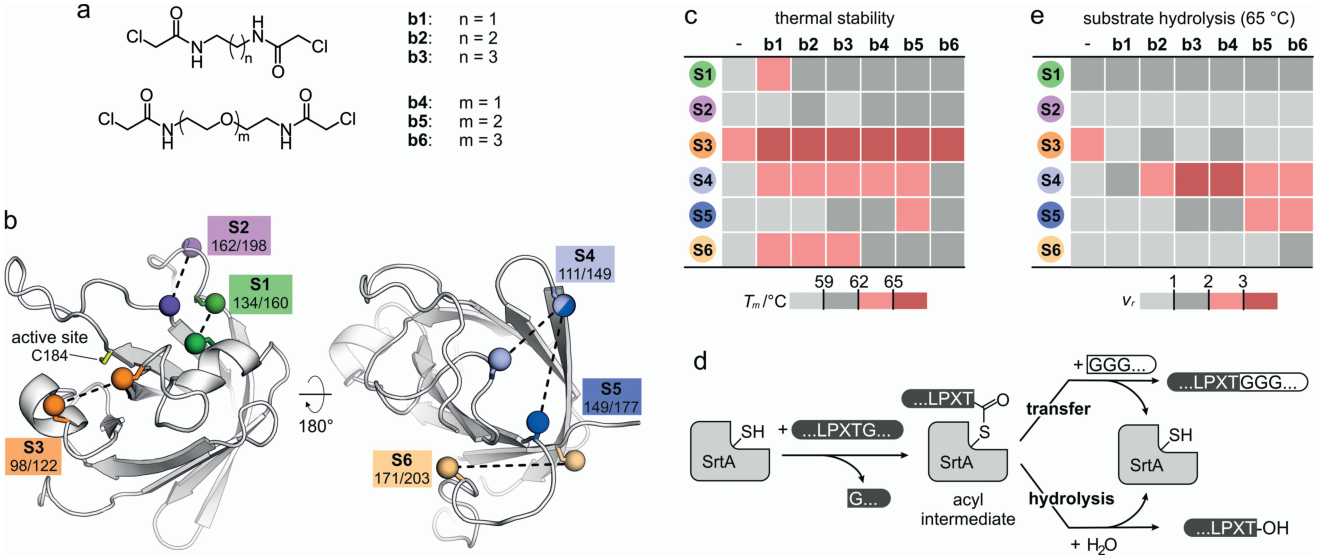

Figure 2. a) Biselectrophiles (**b1**–**b6**) used for the generation of monocyclic enzymes. b) NMR structure of SrtA (PDB: 1ija) with positions of cysteine variations highlighted. Cysteine pairs (same color) and their positions are shown (for details see Figure S3). c) Heat map representation of apparent T_m values (heating rate: 1 °C min^{-1}) for linear and crosslinked SrtA variants (75 μM; for melting curves and apparent T_m values, see Figure S6). d) Mechanism of the SrtA-mediated transpeptidation reaction (recognition motif: LPXTG). e) Heat map representation of enzymatic activity (v_r, relative to wild-type SrtA) of linear and crosslinked SrtA variants at 65 °C (10 μM enzyme, 10 μM fluorescent probe; for v_r values, see Table S2). Buffer for **2c** and **2e**: 20 mM HEPES, pH 7.5, 150 mM NaCl, 5 mM $CaCl_2$, 2 mM TCEP; for **3e**: including 0.01 % Tween 20.

screening, we chose the hydrolysis reaction[16] at 65 °C, where wild-type SrtA shows strongly reduced performance (4 % residual activity; Figure S7). Relative to SrtA ($v_r = 1$; Figure 2e), a number of crosslinked enzymes show increased activity. Surprisingly, the thermostable cyclic versions of **S3** provide reduced enzymatic activity (Figure 2e). In contrast, crosslinked versions of **S4** and **S5** exhibit robust activity enhancements (> twofold; light and dark red, Figure 2e). The overall highest increase in activity was observed for **S4-b3,** which is 3.4-fold more active than SrtA. Taken together, the observed improvements in the activity at 65 °C are moderate, indicating that monocyclization may not be sufficient to convey enough stabilization of the tertiary structure.

To achieve stronger stabilization effects, we aimed for bicyclization of the enzyme. Notably, the two best performing SrtA variants **S4** and **S5** (light and dark blue, Figure 2b) share one variation site (aa 149). Thus we decided to introduce their three cysteine variations simultaneously (aa 111, 149, and 177), resulting in variant **S7** (Figure 3a), which can form a bicyclic protein upon reaction with a triselectrophile. In analogy to bicyclic peptides[17] and mini-proteins,[18] we selected a C_3-symmetric core for our crosslinker, which was modified with three 2-chloroacetamide groups (**t1**; Figure 3b). Triselectrophile **t1** involves 13 bridging atoms, thereby lying between the preferred crosslink ranges of **S4** (**b3/b4**: 10/11 atoms) and **S5** (**b5/b6**: 14/17 atoms). The crosslinking reaction of **S7** and **t1** proceeds efficiently and provides stapled enzyme **S7-t1** (Figure 3b). Analytical HPLC-MS analysis indicates quantitative conversion of **S7**, clearly showing the formation of a product with the expected molecular weight (Figure S8). High-resolution MS analysis of tryptic fragments confirms the modification of the three introduced cysteines, also verifying the unmodified state of C184 (Figure S9, S10, and S11). Importantly, **S7-t1** exhibits strongly increased thermal stability ($T_m = 70.6$ °C; Figure 3c), which is considerably higher than that of SrtA ($\Delta T_m = +11.2$ °C) and of the most active monocyclic protein **S4-b3** ($\Delta T_m = +6.8$ °C). Next, we determined the enzymatic activity of **S7-t1** at 65 °C (Figure 3d). In line with its superior thermal stability, we observed strongly increased enzymatic activity at 65 °C when compared to SrtA (8.7-fold) and **S4-b3** (2.6-fold; Figure 3d).

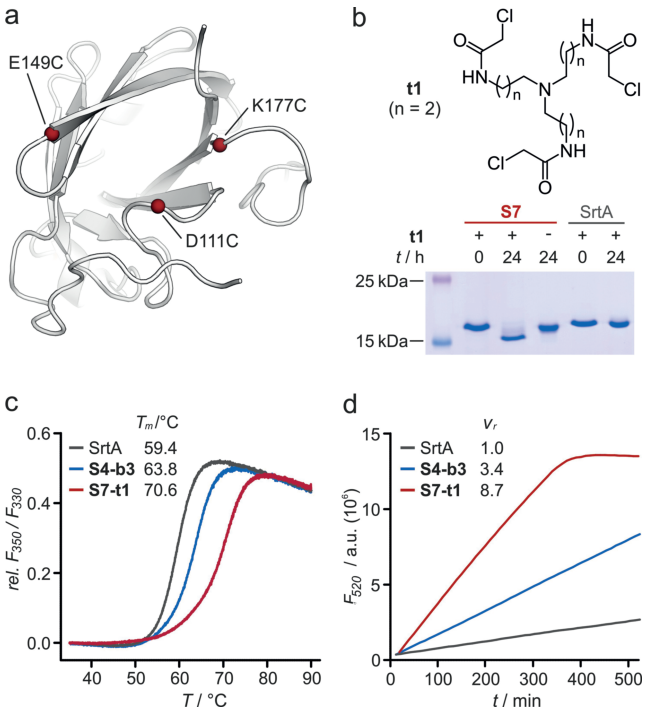

Figure 3. a) NMR structure of SrtA (PDB: 1ija) with positions of cysteine variations in **S7** highlighted. b) Chemical structure of triselectrophile **t1** and Coomassie-stained SDS-PAGE gel showing protein bands after incubation with **t1** (50 μM **S7**, 1 mM **t1**, 50 mM HEPES, pH 8.5, 150 mM NaCl, 5 mM $CaCl_2$, 2 mM TCEP). c) Melting curves of SrtA, **S4-b3**, and **S7-t1** including apparent T_m values (heating rate 1 °C min^{-1}). d) Fluorescence readout of enzymatic activity at 65 °C (10 μM enzyme, 10 μM fluorescent probe). Buffer for **3c** and **3d**: 20 mM HEPES, pH 7.5, 150 mM NaCl, 5 mM $CaCl_2$, 2 mM TCEP, with 0.01 % Tween 20 for (d).

Thus far, we had evaluated enzyme activity under hydrolytic conditions. Envisioning the application of **S7-t1** for protein labeling, we next investigated transpeptidation at 65 °C with the above described fluorescent probe but now in the presence of the nucleophile triglycine (transfer; Figure 2d). Using HPLC-MS as the readout (Figure 4a), we again observed only very low substrate conversion with SrtA (dark gray), similar to a treatment without any enzyme (light gray). In the presence of **S7-t1** (red; Figure 4a), the signal of the starting material (●) was greatly diminished, and two new peaks appeared. Based on the MS (Figure S12), one peak was assigned to the C- (▲) and the other one to the N-terminal fragment (■), which appears to be ligated to triglycine. Importantly, a signal for the hydrolysis product (Dabcyl-QALPET) was not detected, verifying the correct functionality of **S7-t1**. To assess if protein unfolding at elevated temperature is reversible, we compared the enzymatic activity of SrtA and **S7-t1** at 37 °C before and after heating (85 °C, Figure S13). Notably, the transpeptidase activity of both enzymes is not affected by the heating/cooling cycle, indicating reversible unfolding.

Next, we determined the thermal activity profile of the transpeptidation reaction (Figure 4b). Between 37 °C and 55 °C, the activity of SrtA (gray) and **S7-t1** (red) is similar, exhibiting only low temperature dependence. Above 55 °C, both enzymes experience a loss in activity, which is very severe for SrtA, resulting in almost complete inactivation at 65 °C (Figure 4b). For **S7-t1**, the activity reduction is much smaller, with residual activities of 63 % (at 65 °C) and 27 % (at 70 °C) relative to 37 °C. Compared to SrtA, **S7-t1** shows an approximately 10 °C increased tolerance towards thermal stress, which correlates well with its +11.2 °C higher apparent melting temperature. Enhanced thermal stability often goes in hand with a resistance towards denaturants such as guanidinium hydrochloride (GdnHCl). For that reason, the impact of GdnHCl on the transpeptidase activity was investigated (Figure 4c), revealing that the activities of SrtA and **S7-t1** hardly depend on the denaturant concentrations up to 0.5 M. Between 0.75 and 1.5 M, **S7-t1** is significantly more active than SrtA. Most notably, at 1 M GdnHCl, SrtA does not yield any product ($v_r < 1$ %; Figure 4c) while **S7-t1** still provides 40 % residual activity (compared to the absence of

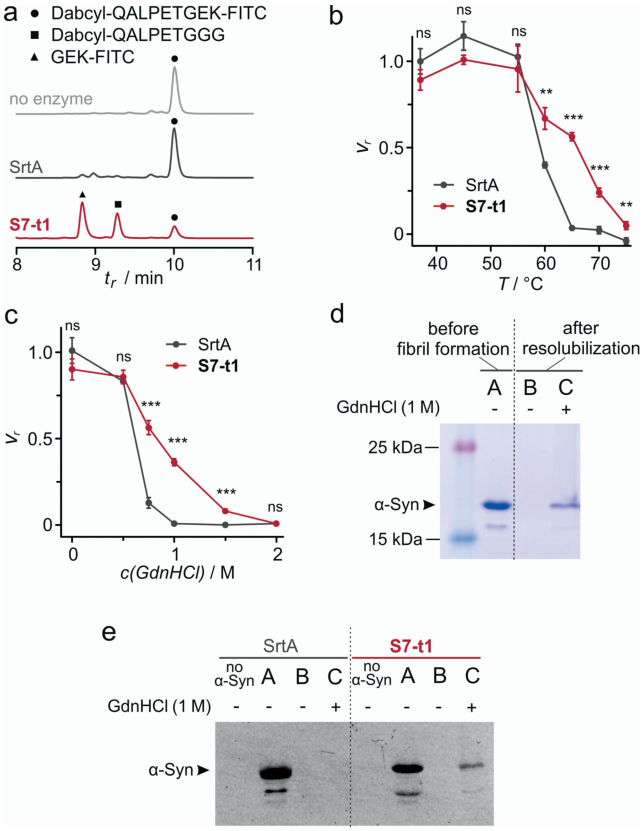

Figure 4. a) HPLC chromatograms (440 nm) of the transpeptidation reaction (12 h at 65 °C) with a fluorescent probe (●) in the absence of enzyme (light gray), with SrtA (dark gray), or with **S7-t1** (red). Product formation (▲, ■) was only observed in the presence of **S7-t1** (50 μM enzyme, 10 μM probe, 2.5 mM GGG; for MS spectra of signals, see Figure S12). b) Temperature dependence of the enzymatic activity (v_i relative to SrtA at 37 °C; 10 μM enzyme, 10 μM probe, 2.5 mM GGG, buffer: 20 mM HEPES, pH 7.5, 150 mM NaCl, 5 mM $CaCl_2$, 2 mM TCEP, 0.01 % Tween 20). Values are mean of triplicate (+/− 1σ, * $p<0.05$, ** $p<0.01$, *** $p<0.001$, ns: not significant). c) Relative enzymatic activity (v_i relative to SrtA in the absence of GdnHCl) at 37 °C for various concentrations of GdnHCl (for details see the Methods Section in the Supporting Information). d) Coomassie-stained SDS-PAGE gel showing the soluble α-Syn fractions before fibril formation (A) and after resolubilization in the absence (B) and presence (C) of GdnHCl (1 M). e) Fluorescence readout ($\lambda_{em}=520$ nm) of α-Syn labeling using soluble fractions before fibril formation A (without GdnHCl) and after re-solubilization B (without GdnHCl) and C (1 M GdnHCl) with either SrtA or **S7-t1** (for details see Figures S14 and S15).

GdnHCl). At higher GdnHCl concentrations (≥2 M), both enzymes are inactive.

Thus far, we had applied **S7-t1** for the labeling of a short test peptide. Next, we were interested whether **S7-t1** would also be useful for protein labeling in particular under conditions where wild-type SrtA does not provide sufficient activity. For that purpose, we chose α-synuclein (α-Syn) as the target. α-Syn comprises 140 amino acids and can form pathogenic fibrils, which are associated with the onset of various neurodegenerative diseases including Parkinson's disease.[19] α-Syn fibrils can be solubilized using GdnHCl.[20] We designed an α-Syn version with a C-terminal SrtA recognition motif (Figure S14) to allow for labeling. Following expression and purification, soluble α-Syn (A) was subjected to fibril formation and ultracentrifugation.[20] Insoluble fibrils were washed and treated with buffer either lacking (B) or containing (C) GdnHCl (1 M).[20] When comparing the resulting soluble fractions (B and C) with the purified and soluble form of α-Syn (A; Figure 4d), we observed resolubilization only in the presence (C) but not in the of absence (B) of GdnHCl. To investigate protein labeling, these soluble samples (A, B, C) were incubated with either SrtA or **S7-t1** and a fluorescent substrate (Figure S14). We then performed analysis by SDS-PAGE employing a fluorescence imager for readout. For soluble α-Syn prior to fibril formation (A), and therefore in the absence of GdnHCl, SrtA and **S7-t1** gave rise to intense bands, indicating efficient protein labeling (Figures 4e and S15). As expected, under resolubilization conditions lacking GdnHCl (B) and therefore also lacking soluble α-Syn, we did not observe any fluorescence signal (B; Figure 4e and S15). On the contrary, for resolubilization with GdnHCl (1 M), α-Syn labeling occurs but only with **S7-t1** and not with wild-type SrtA (C). Notably, differences in the fluorescence band intensities for **S7-t1** (A vs. C; Figure 4e and S15) correlate well with the amount of α-Syn in the soluble fractions (A vs. C; Figure 4d), indicating good labeling efficiencies for **S7-t1** in the presence of GdnHCl.

To assess the broader applicability of protein stabilization by bicyclization, we chose the KIX domain from the human CREB binding protein as a second example (Figure 5a). KIX is an adaptor domain with multiple protein binding partners, such as mixed-lineage leukemia (MLL), and is composed of a central three α-helix bundle (α_1, α_2, α_3). The junction between this bundle and the C-terminal 3_{10} helix (G_1) is crucial for structural integrity (Figure 5a).[21] Thus we focused on this area for tertiary-structure stabilization searching for three positions suitable for cysteine incorporation. Based on our experience with SrtA stabilization, the following guidelines were applied: 1) Solvent-accessible residues were considered that are 2) located in three distinct secondary structures while 3) facing the same side of the protein and 4) spanning a triangle with side lengths between 6 and 17 Å (Cα-Cα distance). Based on these criteria, we selected H594,

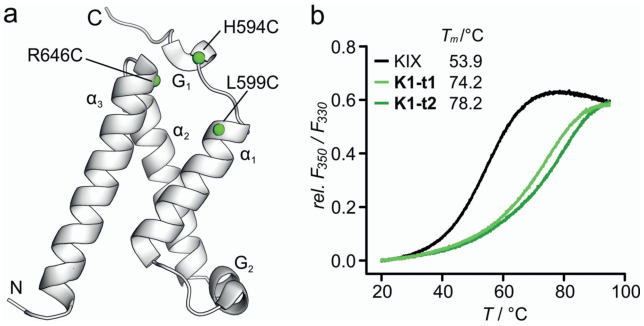

Figure 5. a) NMR structure of KIX (PDB: 2agh), with positions of cysteine variations in **K1** highlighted. The secondary structural elements have been named. b) Melting curves of KIX, **K1-t1**, and **K1-t2**, including apparent T_m values.

L599, and R646 for cysteine introduction, resulting in KIX variant **K1** (Figures 5a and S16).

For crosslinking, we chose triselectrophile **t1** ($n=2$, Figure 3b) and a shorter version **t2** ($n=1$) as we noticed that the distances between the three variation sites in **K1** (7.8, 10.0, and 11.5 Å; Figure S16) are shorter than those in **S7** (8.5, 12.4, and 15.7 Å; Figure S8). The crosslinking with both triselectrophiles proceeds efficiently as confirmed by SDS-PAGE (Figure S17) and HPLC-MS analysis (Figure S18). To evaluate if crosslinking affects the tertiary structure, we compared the affinity of KIX and both bicyclic variants (**K1-t1** and **K1-t2**) to its binding partner MLL (for the sequence see Figure S19). Using a fluorescence polarization assay, similar binding affinities were observed for KIX, **K1-t1**, and **K1-t2** ($K_d=0.6$, 0.9, and 0.9 μM, respectively; Figure S19). Then, we determined apparent melting temperatures (Figure 5b) to find a strongly increased thermal stability for **K1-t1** and **K1-t2** ($\Delta T_m=+20.6$ °C and $+24.6$ °C, respectively) when compared to KIX. Notably, both triselectrophiles have a similar stabilizing effect, with the shorter crosslink **t2** performing best. Based on these results, we were also interested in evaluating the effect of triselectrophile **t2** on SrtA variant **S7**. Again, the crosslinking reaction proceeds efficiently, resulting in bicyclic enzyme **S7-t2** (Figure S20). Notably, we observe a similar thermal stabilization for **S7-t2** ($\Delta T_m=+11.5$ °C, Figure S20) as for **S7-t1** ($\Delta T_m=+11.2$ °C), indicating tolerance towards minor variations in the length of the crosslink.

In summary, we have reported an approach for the in situ cyclization of proteins (INCYPRO) enabling a structure-based stabilization of recombinant proteins that are entirely composed of proteinogenic amino acids. The use of synthetic electrophiles for protein cyclization gives straightforward access to diverse crosslinked architectures with tunable length and flexibility. We applied INCYPRO to generate the bicyclic SrtA variant **S7-t1**, which exhibited strongly increased tolerance towards thermal and chemical denaturation. Importantly, **S7-t1** proved efficient in labeling α-Syn in the presence of 1M GdnHCl. Under these conditions, wild-type SrtA did not show enzymatic activity. From our findings with SrtA, we derived guidelines for the bicyclization and stabilization of proteins and applied them to the KIX domain. A three-cysteine KIX variant was designed and reacted with two different C_3-symmetric triselectrophiles to provide bicyclic KIX versions with up to 24 °C increased thermal stability. In the future, we envision the use of crosslinking agents that allow the introduction of an additional functionality such as an affinity handle (e.g., for enzyme purification/recycling[22] or proximity-assisted enzyme activity[23]). Taken together, the presented protein stabilization technology holds the potential to give rapid access to novel stabilized enzymes, providing an opportunity for the simultaneous incorporation of additional functions.

Acknowledgements

We thank A. Musacchio (MPI Dortmund) for the SrtA expression construct and D. M. Krüger (CGC Dortmund) for a discussion of SrtA variants. We thank F. Müller (MPI Dortmund) for technical support with mass spectrometry. We thank the Deutsche Forschungsgemeinschaft (DFG; Emmy Noether program GR3592/2-1) and the European Research Council (ERC; ERC starting grant 678623). We are grateful for support by AstraZeneca, Bayer CropScience, Bayer HealthCare, Boehringer Ingelheim, Merck KGaA, and the Max Planck Society.

Conflict of interest

The authors declare no conflict of interest.

Keywords: INCYPRO · protein engineering · protein labeling · sortase A · tertiary structure

How to cite: *Angew. Chem. Int. Ed.* **2018**, *57*, 11164–11170
Angew. Chem. **2018**, *130*, 11334–11340

[1] a) U. T. Bornscheuer, G. W. Huisman, R. J. Kazlauskas, S. Lutz, J. C. Moore, K. Robins, *Nature* **2012**, *485*, 185–194; b) C. P. R. Hackenberger, D. Schwarzer, *Angew. Chem. Int. Ed.* **2008**, *47*, 10030–10074; *Angew. Chem.* **2008**, *120*, 10182–10228.

[2] a) A. J. Keefe, S. Jiang, *Nat. Chem.* **2012**, *4*, 59–63; b) J. Milton Harris, R. B. Chess, *Nat. Rev. Drug Discovery* **2003**, *2*, 214–221.

[3] a) M. T. Reetz, *Angew. Chem. Int. Ed.* **2013**, *52*, 2658–2666; *Angew. Chem.* **2013**, *125*, 2720–2729; b) C. Jost, A. Plückthun, *Curr. Opin. Struct. Biol.* **2014**, *27*, 102–112; c) T. J. Magliery, *Curr. Opin. Struct. Biol.* **2015**, *33*, 161–168; d) A. M. Chapman, B. R. McNaughton, *Cell Chem. Biol.* **2016**, *23*, 543–553.

[4] F. Agostini, J. S. Völler, B. Koksch, C. G. Acevedo-Rocha, V. Kubyshkin, N. Budisa, *Angew. Chem. Int. Ed.* **2017**, *56*, 9680–9703; *Angew. Chem.* **2017**, *129*, 9810–9835.

[5] V. S. Dani, C. Ramakrishnan, R. Varadarajan, *Protein Eng. Des. Sel.* **2003**, *16*, 187–193.

[6] N. Martínez-Sáez et al., *Angew. Chem. Int. Ed.* **2017**, *56*, 14963–14967; *Angew. Chem.* **2017**, *129*, 15159–15163.

[7] A. J. Doig, D. H. Williams, *J. Mol. Biol.* **1991**, *217*, 389–398.

[8] A. A. Dombkowski, K. Z. Sultana, D. B. Craig, *FEBS Lett.* **2014**, *588*, 206–212.

[9] a) J. A. Camarero, T. W. Muir, *J. Am. Chem. Soc.* **1999**, *121*, 5597–5598; b) H. Iwai, A. Plu, *FEBS Lett.* **1999**, *459*, 166–172; c) C. Schoene, J. O. Fierer, S. P. Bennett, M. Howarth, *Angew. Chem. Int. Ed.* **2014**, *53*, 6101–6104; *Angew. Chem.* **2014**, *126*, 6215–6218.

[10] a) E. J. Moore, D. Zorine, W. A. Hansen, S. D. Khare, R. Fasan, *Proc. Natl. Acad. Sci. USA* **2017**, *114*, 12472–12477; b) T. Liu, Y. Wang, X. Luo, J. Li, S. A. Reed, H. Xiao, T. S. Young, P. G. Schultz, *Proc. Natl. Acad. Sci. USA* **2016**, *113*, 5910–5915.

[11] J. W. Chin, *EMBO J.* **2011**, *30*, 2312–2324.

[12] a) C. P. Guimaraes, M. D. Witte, C. S. Theile, G. Bozkurt, L. Kundrat, A. E. M. Blom, H. L. Ploegh, *Nat. Protoc.* **2013**, *8*, 1787–1799; b) J. J. Bellucci, J. Bhattacharyya, A. Chilkoti, *Angew. Chem. Int. Ed.* **2015**, *54*, 441–445; *Angew. Chem.* **2015**, *127*, 451–455; c) L. Schmohl, D. Schwarzer, *Curr. Opin. Chem. Biol.* **2014**, *22*, 122–128.

[13] a) H. Jo, N. Meinhardt, Y. Wu, S. Kulkarni, X. Hu, K. E. Low, P. L. Davies, W. F. Degrado, D. C. Greenbaum, *J. Am. Chem. Soc.* **2012**, *134*, 17704–17713; b) A. Muppidi, K. Doi, S. Edwardraja, E. J. Drake, A. M. Gulick, H. G. Wang, Q. Lin, *J. Am. Chem. Soc.* **2012**, *134*, 14734–14737; c) P. Diderich, D. Bertoldo, P. Dessen, M. M. Khan, I. Pizzitola, W. Held, J. Huelsken, C. Heinis, *ACS Chem. Biol.* **2016**, *11*, 1422–1427;

d) A. M. Spokoyny, Y. Zou, J. J. Ling, H. Yu, Y. S. Lin, B. L. Pentelute, *J. Am. Chem. Soc.* **2013**, *135*, 5946 – 5949; e) M. R. Jafari, L. Deng, P. I. Kitov, S. Ng, W. L. Matochko, K. F. Tjhung, A. Zeberoff, A. Elias, J. S. Klassen, R. Derda, *ACS Chem. Biol.* **2014**, *9*, 443 – 450; f) M. Pelay-Gimeno, A. Glas, O. Koch, T. N. Grossmann, *Angew. Chem. Int. Ed.* **2015**, *54*, 8896 – 8927; *Angew. Chem.* **2015**, *127*, 9022 – 9054.

[14] a) N. Brauckhoff, G. Hahne, J. T. H. Yeh, T. N. Grossmann, *Angew. Chem. Int. Ed.* **2014**, *53*, 4337 – 4340; *Angew. Chem.* **2014**, *126*, 4425 – 4429; b) C. Stiller, D. M. Krüger, N. Brauckhoff, M. Schmidt, P. Janning, H. Salamon, T. N. Grossmann, *ACS Chem. Biol.* **2017**, *12*, 504 – 509.

[15] a) U. Ilangovan, H. Ton-That, J. Iwahara, O. Schneewind, R. T. Clubb, *Proc. Natl. Acad. Sci. USA* **2001**, *98*, 6056 – 6061; b) Y. Zong, T. W. Bice, H. Ton-That, O. Schneewind, S. V. L. Narayana, *J. Biol. Chem.* **2004**, *279*, 31383 – 31389.

[16] a) B. C. Chenna, J. R. King, B. A. Shinkre, A. L. Glover, A. L. Lucius, S. E. Velu, *Eur. J. Med. Chem.* **2010**, *45*, 3752 – 3761; b) K. B. Oh, S. H. Kim, J. Lee, W. J. Cho, T. Lee, S. Kim, *J. Med. Chem.* **2004**, *47*, 2418 – 2421.

[17] a) P. Timmerman, J. Beld, W. C. Puijk, R. H. Meloen, *ChemBioChem* **2005**, *6*, 821 – 824; b) C. Heinis, T. Rutherford, S. Freund, G. Winter, *Nat. Chem. Biol.* **2009**, *5*, 502 – 507; c) S. Chen, D. Bertoldo, A. Angelini, F. Pojer, C. Heinis, *Angew. Chem. Int. Ed.* **2014**, *53*, 1602 – 1606; *Angew. Chem.* **2014**, *126*, 1628 – 1632.

[18] B. Dang, H. Wu, V. K. Mulligan, M. Mravic, Y. Wu, T. Lemmin, A. Ford, D.-A. Silva, D. Baker, W. F. DeGrado, *Proc. Natl. Acad. Sci. USA* **2017**, *114*, 10852 – 10857.

[19] M. R. Cookson, *Mol. Neurodegener.* **2009**, *4*, 9.

[20] R. Porcari et al., *J. Biol. Chem.* **2015**, *290*, 2395 – 2404.

[21] R. N. De Guzman, N. K. Goto, H. J. Dyson, P. E. Wright, *J. Mol. Biol.* **2006**, *355*, 1005 – 1013.

[22] C. B. Rosen, R. L. Kwant, J. I. MacDonald, M. Rao, M. B. Francis, *Angew. Chem. Int. Ed.* **2016**, *55*, 8585 – 8589; *Angew. Chem.* **2016**, *128*, 8727 – 8731.

[23] H. H. Wang, B. Altun, K. Nwe, A. Tsourkas, *Angew. Chem. Int. Ed.* **2017**, *56*, 5349 – 5352; *Angew. Chem.* **2017**, *129*, 5433 – 5436.

Manuscript received: April 17, 2018
Accepted manuscript online: May 30, 2018
Version of record online: June 21, 2018

